

CHAPTER 3

WAVEFRONT RECONSTRUCTION METHODS

Pierce [9] defines a wavefront as “any moving surface along which a waveform feature is being simultaneously received.” The first step in performing ray tracing is determining these wavefronts from the time-domain pressure waveforms over the computational domain. Once these waveforms have been computed, one can then proceed to compute the normals and intersections to propagate the rays. Wavefront computation is also the step most prone to errors. These errors are usually the result of multiple reflections or attenuation at interfaces. Multiple approaches to wavefront reconstruction are presented here along with a discussion of how well they are able to handle the various pitfalls of wavefront reconstruction methods.

All of the methods presented here make the same assumptions about the data being used. The data are assumed to have originated from some sort of computational simulation over a uniform square spatial grid in three dimensions with N points per dimension separated by a distance $dx = dy = dz$. Each point (x, y, z) on the grid is assumed to have a time-domain pressure waveform associated with it, denoted as $p(x, y, z, t)$. The source of excitation is assumed to be a finite duration tone pulse $p_{ref}(t)$, although most methods can be used for any finite duration pulse with minor modifications. The incident field is assumed to be a plane wave propagating in the $+z$ direction.

3.1 Spatial Correlation

3.1.1 Method

The idea behind the spatial correlation method is to determine the wavefront at a time τ by finding the z coordinate for each (x, y) pair that maximizes the correlation of $p(x, y, z, t)$ and $p_{ref}(t - \tau)$.

3.1.2 Issues

Strong scatterers cause this method to fail due to reduction in the pulse's magnitude. Assume that $p(x, y, z, t)$ is equal to a time-delayed and scaled version of p_{ref} and the excitation is a tone burst. Consider a point (x_0, y_0, z_0) that is the actual wavefront at time t and some other point (x_1, y_1, z_1) . Let $p(x_1, y_1, z_1, t) = A_0 p(x_0, y_0, z_0, t - nT)$, where T is the reciprocal of the center frequency of the tone burst, n is an integer, and A_0 is a result of the attenuation due to transmission loss. If A_0 is sufficiently small, it is possible that although the shifted reference pulse is not perfectly aligned with $p(x_1, y_1, z_1, t)$, it will still have a larger correlation with $p_{ref}(t)$ than will $p(x_0, y_0, z_0, t)$. As a result, the wavefront will be incorrectly identified as being located at (x_1, y_1, z_1) instead of (x_0, y_0, z_0) .

This method solves for the wavefront directly, but the methods to follow will determine the wavefront indirectly. Instead of finding the wavefront at time τ , the time it takes for the pulse to reach (x, y, z) is determined. The wavefront at a time τ is then the set of (x, y, z) with the same pulse arrival time. This indirect method of determining wavefronts generally is less vulnerable to attenuation as will be explained in the next section.

3.2 Temporal Correlation

3.2.1 Method

The temporal correlation method, like the spatial correlation method, assumes that $p(x, y, z, t)$ is a delayed version of $p_{ref}(t)$. The arrival time τ of the pulse at a position (x, y, z) is then computed by finding the value of τ that maximizes the correlation of $p(x, y, z, t)$ with $p_{ref}(t - \tau)$. Since the magnitudes of both signals being compared do not change from one delay to another, the attenuation issue encountered with the spatial correlation method is no longer a problem. This particular method works quite well when applied to weak scatterers since the assumption that the $p(x, y, z, t)$ is approximately a time delayed version $p_{ref}(t)$ holds.

3.2.2 Example

The reference signal p_{ref} is plotted in Fig. 3.1 and the pressure at a location (x, y, z) is shown in Fig. 3.2. The correlation of $p(x, y, z, t)$ with time-shifted versions of $p_{ref}(t)$ and is plotted in Fig. 3.3. The time-shift corresponding to the largest correlation value is -0.6472 ms. Figure 3.4 shows p_{ref} shifted by -0.6472 ms with $p(x, y, z, t)$. The incident waveform and the shifted reference signal line up correctly and therefore the arrival time was computed correctly.

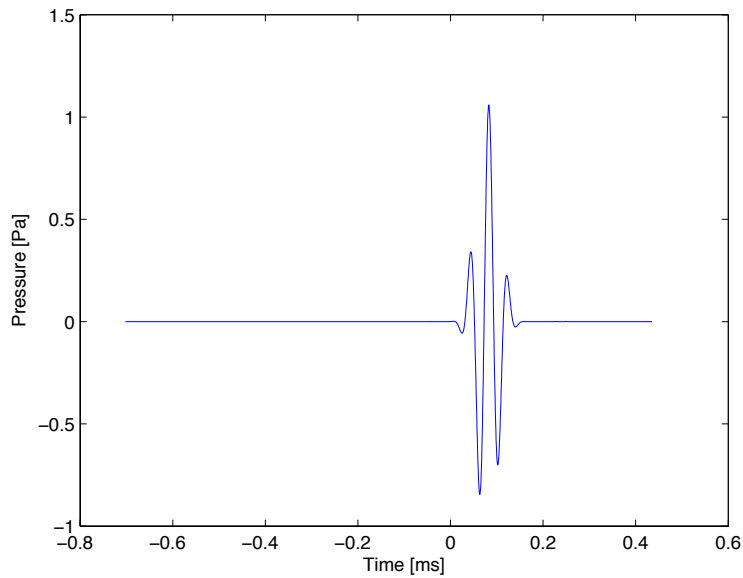


Figure 3.1: Reference signal p_{ref} .

3.2.3 Issues

Reflections and interference can cause significant errors in the results obtained with this method.

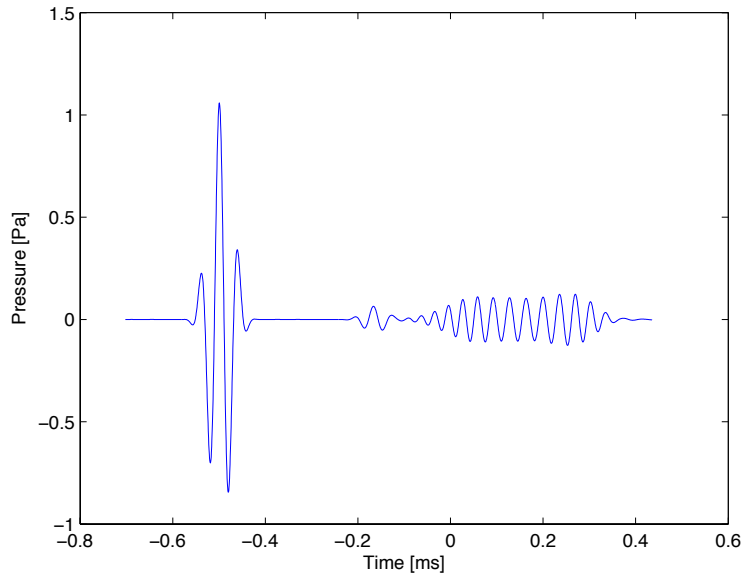


Figure 3.2: Pressure signal for temporal correlation example.

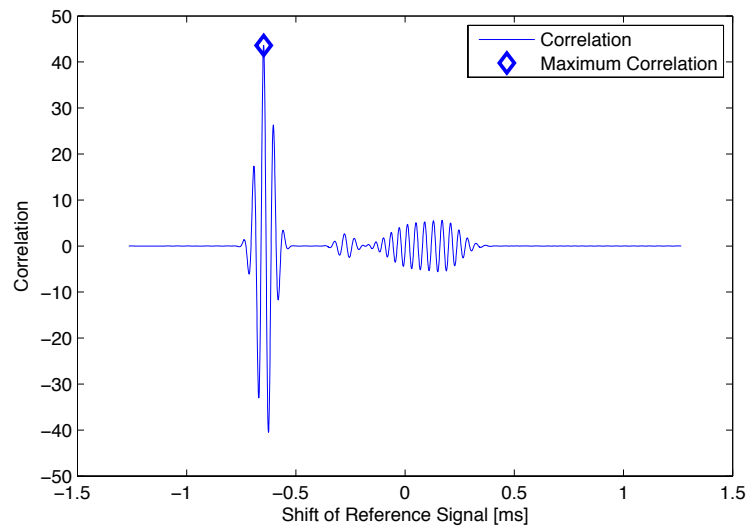


Figure 3.3: Correlation of pressure signal from Fig. 3.2 and time-shifted versions of p_{ref} . The maximum correlation point is marked with a diamond and corresponds to a time shift of -0.6472 ms.

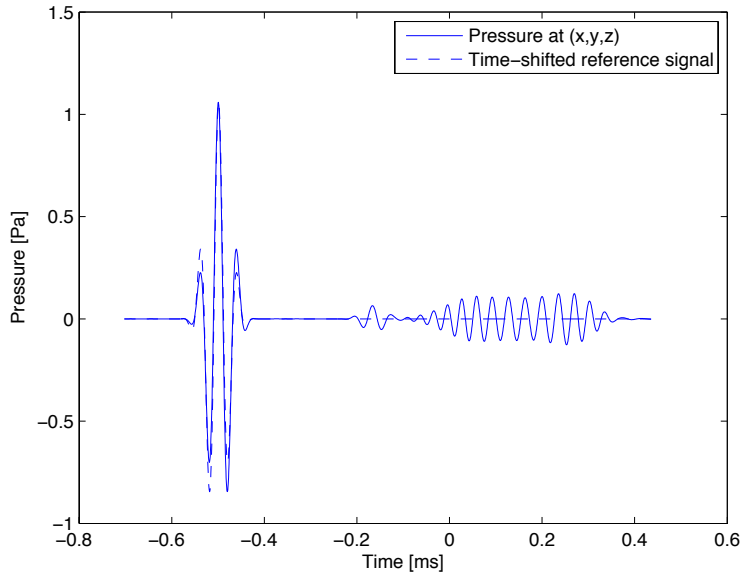


Figure 3.4: Pressure signal from Fig. 3.2 and time-shifted version of reference signal computed using temporal correlation method.

3.3 Minimum Weighted Phase Error

3.3.1 Method

The idea behind the minimum weighted phase error method is observation that the delay of a single frequency component of a signal can be determined by the phase of the Fourier transform of a signal at that frequency. Another observation is that the influence of each frequency component is proportional to the magnitude of the Fourier transform at that frequency. Assume that the $p(x, y, z, t)$ is approximately a time delayed version of $p_{ref}(t)$ after being run through some filter with a phase response of zero. Let $P(x, y, z, f)$ be the Fourier transform of $p(x, y, z, t)$ and $P_{ref}(\tau, f)$ be the Fourier transform of $p_{ref}(t - \tau)$. Define the weighted phase error function $e_\theta(\tau, f)$ as

$$e_\theta(\tau, f) = |\angle P(x, y, z, f) - \angle P_{ref}(\tau, f)| |P(x, y, z, f)| \quad (3.1)$$

The pulse arrival time at the point (x, y, z) is then the value of τ that minimizes the integral of the weighted phase error function over all frequencies.

In equation form,

$$\tau = \underset{t}{\operatorname{argmin}} \left\{ \int_{-\infty}^{\infty} e_{\theta}(t, f) df \right\} \quad (3.2)$$

3.3.2 Issues

Computation of the unwrapped phase is still an unsolved problem, so the phase computation in Eq. (3.1) is done with the wrapped phase. This can result in a computed phase error that can be either greater or less than the actual value. For example, if $\angle P(x, y, z, f) = 0.99\pi$ the wrapped phase of $p_{ref}(\tau, f)$ is -0.99π , the phase error computed will be 1.98π while the actual phase error is 0.02π since a wrapped phase of -0.99π is equivalent to a phase of 1.01π . On the other hand, if the unwrapped phase of $p(x, y, z, f)$ is 4.1π and the unwrapped phase of $p_{ref}(\tau, f)$ is 2.1π , the unwrapped phase error is 2π while the wrapped phase error is 0. This last point results in significant error in the phase error computation and often results in maxima of $e_{\theta}(\tau, f)$ occurring at the actual arrival time and also at the arrival time offset by integer multiples of the pitch period for tone burst stimulation.

3.4 Peak Detection

3.4.1 Method

The peak detection uses the first peak of the pulse to be the waveform feature that is tracked over time. The advantage of using the first peak is that this peak is least likely to be distorted by interference patterns. The method works as follows. Set some threshold pressure p_{thr} to be the minimum pressure amplitude that will be considered a peak. This parameter should be chosen so that any noise occurring before the arrival of the pulse is not detected as a peak. Then for a point (x, y, z) find the first t that satisfies $p(x, y, z, t) \geq p_{thr}$. This time will be denoted as t_{thr} . The arrival time τ is then the next local maxima in $p(x, y, z, t)$ such that $\tau \geq t_{thr}$.

3.4.2 Example

Consider the pressure signal at a point (x, y, z) shown in Fig. 3.5. A value of $p_{thr} = 0.15$ is plotted as the dotted line in the figure. The first peak greater than p_{thr} occurs at the point marked by the diamond in the figure. This corresponds to an arrival time of -0.538 ms.

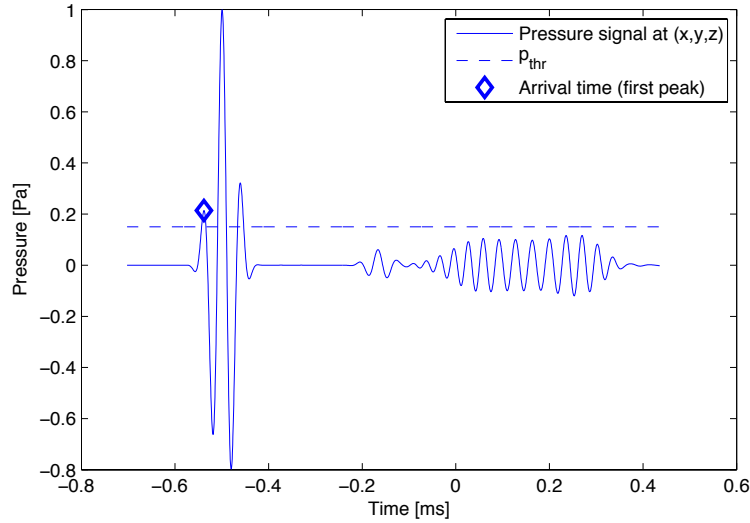


Figure 3.5: Example signal used for the peak detection method. The signal observed at the point (x, y, z) is shown as the solid line, the threshold pressure p_{thr} is the dotted line, and the arrival time is marked by the diamond at -0.538 ms.

3.4.3 Issues

Peaks introduced by noise can result in a false detection of the first peak. If this becomes an issue, a simple solution is to multiply the pressure waveform by its envelope. This will also reduce the magnitude of the first peak, but this reduction will be less than the the reduction of the noise outside of the pulse. It should also be noted that due to attenuation, the $p(x, y, z, t)$ should be normalized to have a maximum of 1 and p_{thr} then becomes the ratio of the noise maximum to the pulse maximum.

3.5 Previous Sample Temporal Correlation

3.5.1 Method

This method is based on the assumption that $p(x, y, z, t)$ is more like a delayed version of $p(x, y, z - dz, t)$ than $p_{ref}(t)$. This is usually the case, especially when multiple reflections occur. The method is similar to the temporal correlation method except that the correlation is now taken between $p(x, y, z, t)$ and $p(x, y, z - dz, t)$. The difference in arrival times between $z - dz$ and z is then computed by finding the delay τ of $p(x, y, z - dz, t)$ that maximizes the correlation with $p(x, y, z, t)$. Denote this delay as $\tau_{max}(x, y, z)$. This method is recursive since in order to find the arrival time at a position (x, y, z) , the delays from all of the previous z values must be summed.

$$\tau(x, y, z) = \sum_{n=\min\{z\}/dz}^{z/dz} \tau_{max}(x, y, ndz) \quad (3.3)$$

3.5.2 Example

The signals at (x, y, z) and $(x, y, z - dz)$ are shown in Fig. 3.6. The correlation of $p(x, y, z, t)$ with time shifted versions of $p(x, y, z - dz, t)$ is shown in Fig. 3.7 with a maximum at a time shift of $9.443 \mu\text{s}$. The pressure at (x, y, z) is plotted with the pressure at $(x, y, z - dz)$ shifted by $9.443 \mu\text{s}$ in Fig. 3.8. As can be seen from the figure, the shifted version $p(x, y, z - dz, t)$ is aligned with $p(x, y, z, t)$.

3.5.3 Issues

The recursive nature of the method has the drawback that an error in one delay computation for a given (x_0, y_0, z_0) coordinate results in an error in the arrival time for all (x_0, y_0, z) for $z \geq z_0$. Reflections also introduce error, although of a smaller magnitude than the error encountered for the previous correlation based methods. This error results from the fact that when the incident pulses are maximally correlated, the reflected pulses will be slightly out of phase due to their differing path lengths. This correlation of the reflected pulses causes the delay estimate to be less than the actual delay.

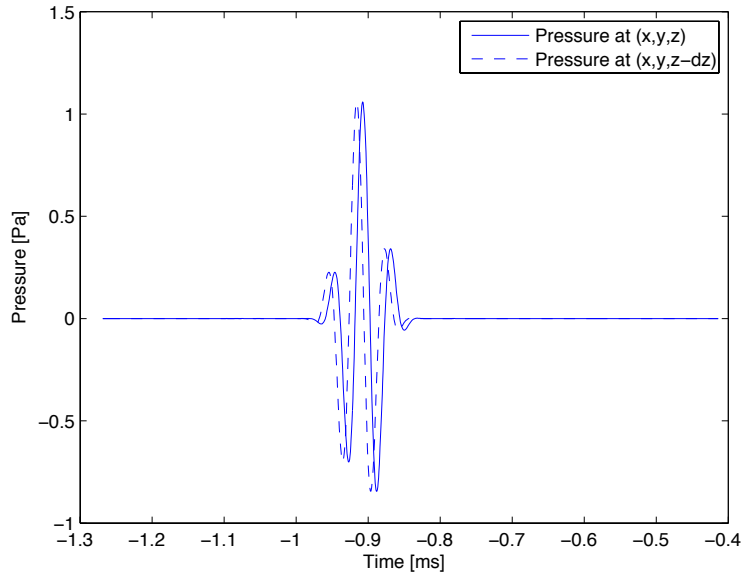


Figure 3.6: Pressure signals at (x, y, z) (solid line) and at $(x, y, z - dz)$ (dashed line).

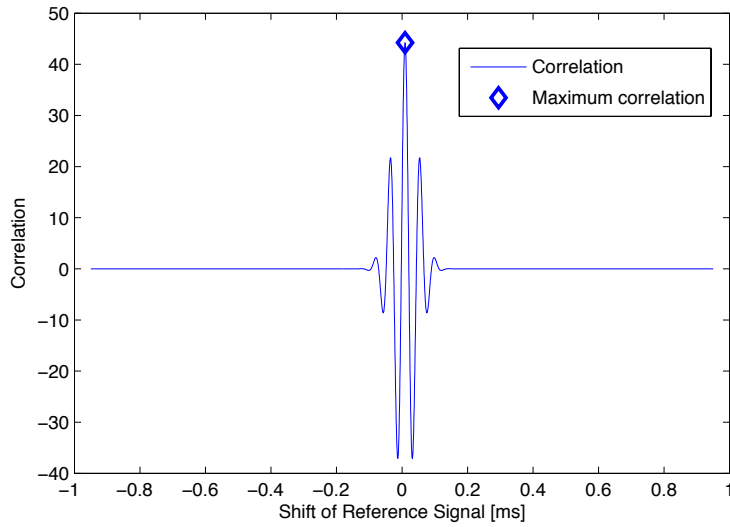


Figure 3.7: Cross-correlation of pressure signal at (x, y, z) with pressure signal at $(x, y, z - dz)$. The diamond indicates the maximum correlation which occurs at a time of $9.443 \mu\text{s}$.

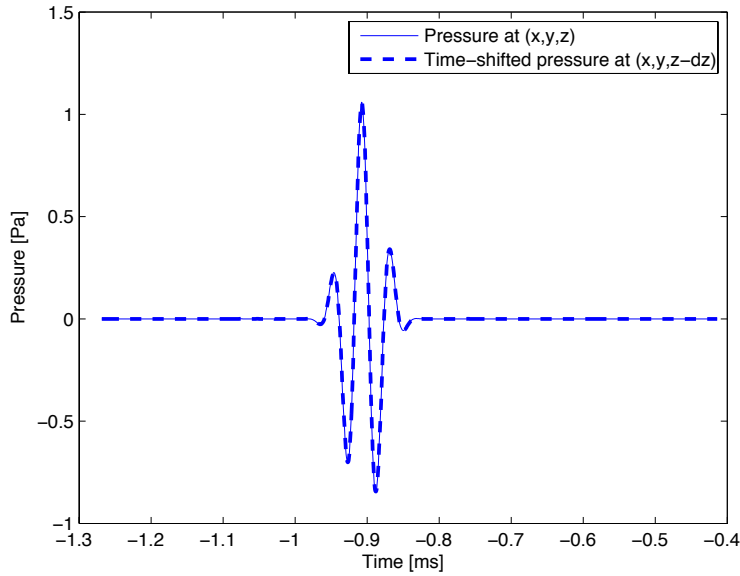


Figure 3.8: $p(x, y, z-dz, t)$ Shifted by the amount found using the last sample temporal correlation method (dashed line) and $p(x, y, z, t)$ (solid line).

The severity of this effect is proportional to the ratio of the magnitude of the reflected pulse to the magnitude of the incident pulse. An example of this is shown in Figs. 3.9-3.11. Figure 3.9 shows $p(x, y, z, t)$ and $p(x, y, z - dz, t)$ when a strong reflected pulse is present. Figure 3.10 shows the cross-correlation of the two signals with a maximum correlation occurring for a shift of $2.518 \mu\text{s}$. Figure 3.11 shows $p(x, y, z - dz, t)$ shifted by the value computed with the method and $p(x, y, z, t)$. Looking closely at the figure, it can be seen that the reflected pulse is aligned while the incident pulse is slightly out of phase.

3.6 Previous Sample Temporal Correlation with First Peak Alignment Correction

3.6.1 Method

This method combines the peak detection method with the previous sample temporal correlation method to improve the method's ability to compensate

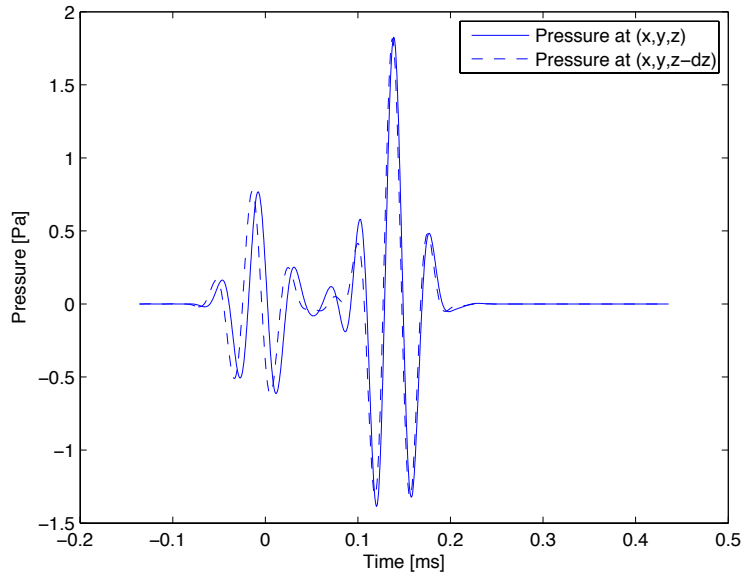


Figure 3.9: Pressure signals at (x, y, z) (solid line) and at $(x, y, z - dz)$ (dashed line) with reflections.

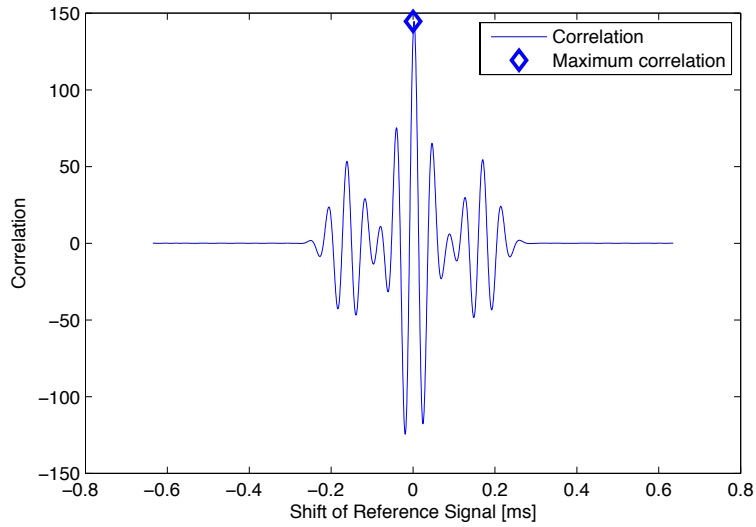


Figure 3.10: Cross-correlation of pressure signal at (x, y, z) with pressure signal at $(x, y, z - dz)$ with reflections. The diamond indicates the maximum correlation which occurs at a time of $2.518 \mu s$.

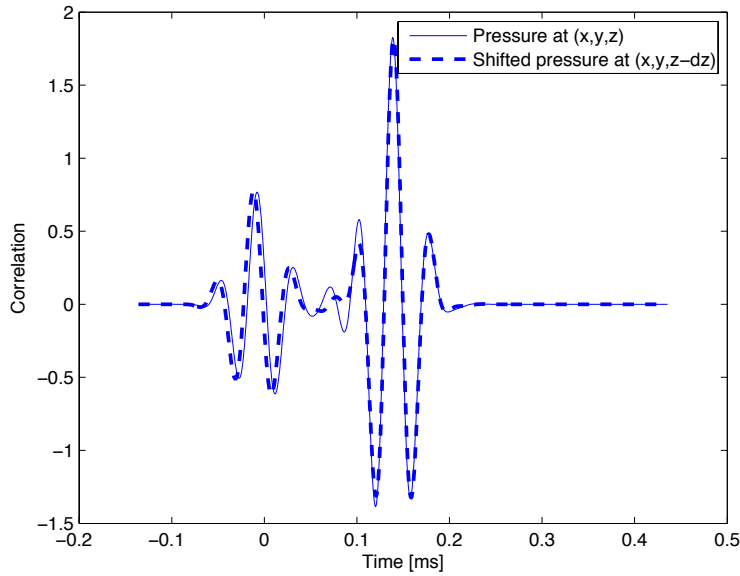


Figure 3.11: $p(x, y, z - dz, t)$ Shifted by the amount found using the last sample temporal correlation method (dashed line) and $p(x, y, z, t)$ (solid line) with reflections.

for noise and interference. The first step is to perform the previous sample temporal correlation method to get a rough estimate of the arrival time. The peak detection method is then applied subject to the constraint that the absolute difference in arrival times from $(x, y, z - dz)$ and (x, y, z) must be less than some maximum delay. In this case, the maximum delay is the maximum time it should take to travel a distance of dz multiplied by some tolerance factor greater than 1. If c_{min} is the minimum sound speed over the domain and A_{tol} is the tolerance factor, the maximum delay τ_{max} is then

$$\tau_{max} = \frac{A_{tol}dz}{c_{min}} \quad (3.4)$$

If the delay is not within this tolerate range, the previous sample temporal correlation method is used to approximate the delay between the last sample and the current sample.

3.6.2 Issues

This method results in more accurate arrival determination than either of the methods used on their own. When the first peak method fails and the previous sample temporal correlation must be used, the solution is not exact but is more accurate than would be found using the first peak method. One issue arises as a result of the use of the previous sample temporal correlation method. Since this method has a tendency to underestimate the actual delay, if used on enough samples in a row, the peak detection method may be detected as outside of the allowed delay when the correct arrival time was found.